Miniaturized Wideband Bandpass Filter based on Capacitor-loaded One-eighth Wavelength Coupled Line

Jin Shi [1,2,3], Jiancheng Dong [1], Kai Xu [1,2,3], and Lingyan Zhang [1,2,3]

[1] School of Information Science and Technology
Nantong University, Nantong, 226019, China
jinshi0601@hotmail.com, Dongjiancheng2019@outlook.com, xukaihopeness@ hotmail.com, zhangly@ntu.edu.cn

[2] Nantong Research Institute for Advanced Communication Technologies
Nantong, 226019, China

[3] Research Center for Intelligent Information Technology
Nantong University, Nantong, 226019, China

Abstract ─ A novel miniaturized wideband bandpass filter (BPF) using capacitor-loaded microstrip coupled line is proposed. The capacitors are loaded in parallel and series to the coupled line, which makes the filter just require one one-eighth wavelength coupled line and achieve filtering response with multiple transmission poles (TPs) and transmission zeros (TZs). Compared with the state-of-the-art microstrip wideband BPFs, the proposed filter has the advantages of compact size and simple structure. A prototype centered at 1.47 GHz with the 3-dB fractional bandwidth of 86.5% is demonstrated, which exhibits the compact size of $0.003\lambda_g^2$ (λ_g is the guided wavelength at the center frequency) and the minimum insertion loss of 0.37 dB.

Index Terms ─ Bandpass filter, capacitors, coupled line, miniaturized, wideband.

I. INTRODUCTION

Miniaturized wideband bandpass filter (BPF) is one essential component in the modern wireless communication system owing to the advantages of compact size and high date-rate transmissions. So far, numerous microstrip wideband BPFs have been proposed based on various structure, including stub-loaded multiple-mode resonator [1]-[6], stub-loaded coupled line [7]-[9], cross-coupled multiple-mode resonator [10], ring resonator associated with open stubs [11]-[12], and stub-loaded stepped impedance resonator (SIR) [13]-[16]. However, the filter utilizing the above structures suffers from the large circuit size (e.g., $0.271\lambda_g^2$), which is mainly derived from the large size of the resonator or extra loaded stubs.

In order to reduce the size of microstrip wideband BPF, quarter-wavelength three-line coupled structure [17], high-impedance microstrip line with folded stepped impedance stubs and radial stubs [18], and quarter-wavelength interdigital coupled SIR [19] are utilized. The circuit size can be reduced to $0.013\lambda_g^2$, $0.009\lambda_g^2$, and $0.006\lambda_g^2$, respectively, but with a complex structure.

Loading lumped elements can also help reduce the circuit size of microstrip BPF. For instance, capacitors are loaded in parallel on the half-wavelength microstrip coupled line so that a miniaturized differential wideband BPF [20] can be achieved.

In this letter, four capacitors are loaded in parallel and series to just one one-eighth wavelength microstrip coupled line. The filter size can be further reduced, and the filter structure becomes much simpler. Wideband filtering response and out-of-band suppression are ensured by three transmission poles (TPs) and four transmission zeros (TZs), which are produced and controlled by capacitances and loading positions of capacitors as well as the even-odd-mode impedance of the coupled line. Odd- and even-mode analysis is utilized for theoretical analysis. One prototype is designed for demonstration.

II. PROPOSED WIDEBAND BANDPASS FILTER

The circuit model of the proposed wideband BPF is exhibited in Fig. 1 (a), which is composed of four capacitors (C_1, C_2, and C_3), one one-eighth wavelength coupled line with its one end shorted (Z_e and Z_o, $\theta_1+\theta_2 = 45°$), and two ports (Port 1 and Port 2). C_1 is loaded in series to the coupled line. C_2 and C_3 are loaded in parallel to the coupled line. C_1 and C_2 are located at the open end of the coupled line. The electrical distance between C_2 and C_3 is θ_1.

Submitted On: December 23, 2020
Accepted On: April 18, 2021

https://doi.org/10.47037/2021.ACES.J.360707

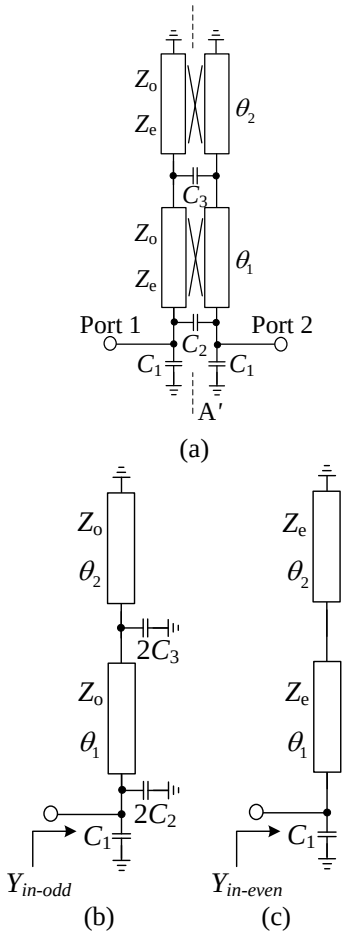

Fig. 1. Circuit model and even- and odd-mode equivalent circuits of the proposed wideband BPF. (a) Circuit model; (b) even-mode equivalent circuit; (c) odd-mode equivalent circuit.

The whole circuit is symmetrical to the A-A' plane, so odd- and even-mode analysis can be utilized. A virtual open/short appear along the symmetrical plane A-A' under the condition of even/odd-mode operation. Thus, the even- and odd-mode equivalent circuits are shown in Figs. 1 (b) and 1 (c), respectively. The input admittance of even-/odd-mode equivalent circuits can be extracted as:

$$Y_{in-even} = C_1\omega j - \frac{\cot(\theta_1+\theta_2)\,j}{Z_e}, \tag{1a}$$

$$Y_{in-odd} = C_1\omega j + 2C_2\omega j + \frac{2Z_oC_3\omega j + j\tan\theta_1 - j\cot\theta_2}{Z_o + (Z_o\cot\theta_2 - 2Z_o^2C_3\omega j)\tan\theta_1}, \tag{1b}$$

respectively, where $\omega = 2\pi f$,

$$\theta_1+\theta_2 = \frac{\pi}{4}\frac{f}{f_0}, \tag{2}$$

where f_0 is the center frequency. The reflection coefficients (S_{11} and S_{22}) and transmission coefficients (S_{21} and S_{12}) of the proposed design can be derived as:

$$S_{11} = S_{22} = \frac{Y_0^2 - Y_{in-odd}Y_{in-even}}{(Y_0+Y_{in-odd})(Y_0+Y_{in-even})}, \tag{3a}$$

$$S_{21} = S_{12} = \frac{Y_0(Y_{in-odd} - Y_{in-even})}{(Y_0+Y_{in-odd})(Y_0+Y_{in-even})}, \tag{3b}$$

where Y_0 = 1/50 Ω^{-1} is the port admittance. According to Equations (1)-(3), the curves of $|S_{11}|$ and $|S_{21}|$ can be obtained in MATLAB by setting a certain initial value for C_1, C_2, C_3, θ_1/θ_2, and Z_e/Z_o. The frequency corresponding to the extreme point of $|S_{11}|$ curve is the frequency of the TPs, and the frequency corresponding to the extreme point $|S_{21}|$ curve is the frequency of the TZs. Then, TPs and TZs can be obtained.

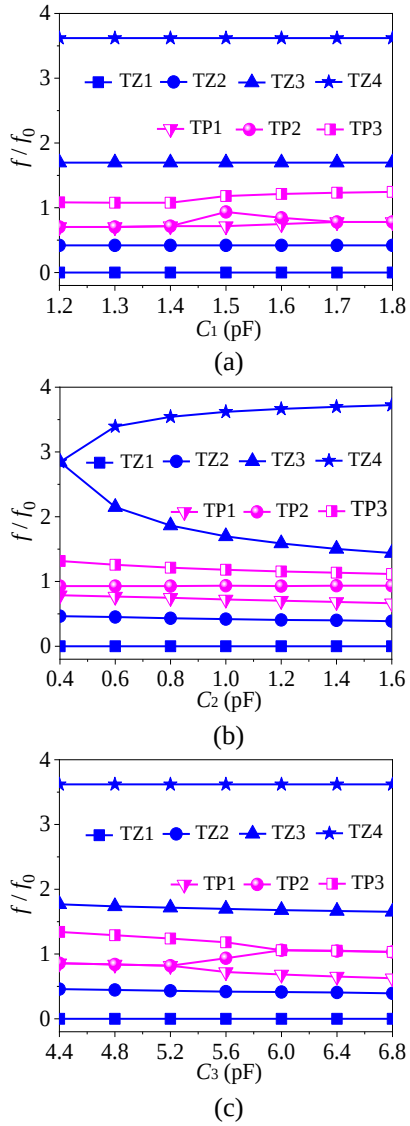

Fig. 2. Effect of capacitance values on theoretical variations of TPs and TZs. (a) C_1 changes; (b) C_2 changes; (c) C_3 changes. (C_1 = 1.5 pF, C_2 = 1.0 pF, C_3 = 5.6 pF, θ_1/θ_2 = 1 and Z_e/Z_o = 1.6).

A. Analysis of TPs and TZs

Figure 2 shows how C_1, C_2, C_3 affect theoretic TPs and TZs. Figure 3 exhibits how θ_1/θ_2 and Z_e/Z_o affect theoretic TPs and TZs. It can be found from Figs. 2 and 3 that TP1 moves upwards when C_1, θ_1/θ_2, or Z_e/Z_o is increased, or C_2 or C_3 is decreased. TP2 moves downwards with the decrease of C_3 or the increase of Z_e/Z_o, while TP2 moves upwards first then moves downwards with C_1. TP3 moves upwards with the increase of C_1 or Z_e/Z_o, or the decrease of C_2, C_3, or θ_1/θ_2. TZ3 moves downwards when C_2 or θ_1/θ_2 increases, or Z_e/Z_o decreases. TZ4 moves upwards with C_2.

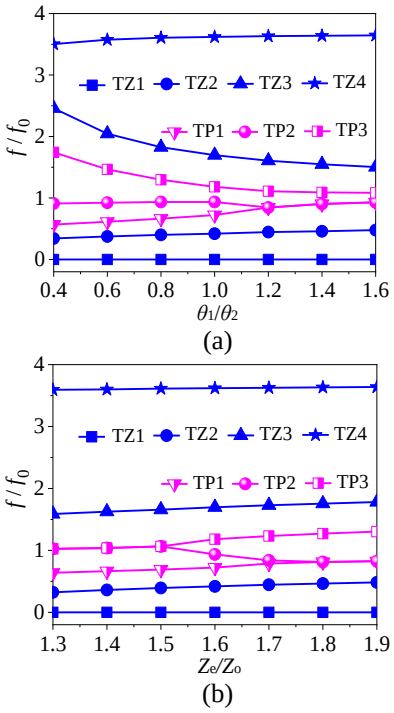

Fig. 3. Effect of loading position of capacitor and impedance of coupled line on theoretical variations of TPs and TZs. (a) θ_1/θ_2 changes; (b) Z_e/Z_o changes. (C_1 = 1.5 pF, C_2 = 1.0 pF, C_3 = 5.6 pF, θ_1/θ_2 = 1 and Z_e/Z_o =1.6).

In addition, the number of TPs changes from three to two when C_1, C_3, θ_1/θ_2, or Z_e/Z_o is outside a special range, while the number of TZs changes from four to three when C_2 is outside a special range. It can be found from Figs. 2 and 3 that three TPs and four TZs can be obtained when selecting appropriate parameters, which ensures wideband filtering response and enough out-of-band suppression for the proposed filter.

It is found that TZs will be affected by C_2 and C_3 but not by C_1. This is because C_2 and C_3 could provide additional transmission paths beside the transmission path of the coupled line, and the signals on the paths will be cancelled each other when the phase difference is (2n+1)180 degrees (n = 0, 1, 2…). However, C_1 doesn't provide an additional path so that it will not affect TZs.

B. Analysis of bandwidth and center frequency

The bandwidth and center frequency can also be obtained from $|S_{11}|$ and $|S_{21}|$ curves in MATLAB. By this way, the effect of C_1, C_2, C_3, θ_1/θ_2, and Z_e/Z_o on bandwidth and center frequency are exhibited in Figs. 4 and 5, respectively. It can be seen from Figs. 4 and 5 that the bandwidth and center frequency are mainly controlled by C_2, C_3, θ_1/θ_2, and Z_e/Z_o. The 3-dB fractional bandwidth (FBW) increases when C_2, θ_1/θ_2, or Z_e/Z_o is decreased, or C_3 is increased. The center frequency moves upwards when C_2, C_3, or θ_1/θ_2 is decreased, or Z_e/Z_o is increased. In addition, the variations of bandwidth and center frequency in Figs. 4 and 5 are consistent with those of the space between the TPs and the position of TPs in Figs. 2 and 3, respectively.

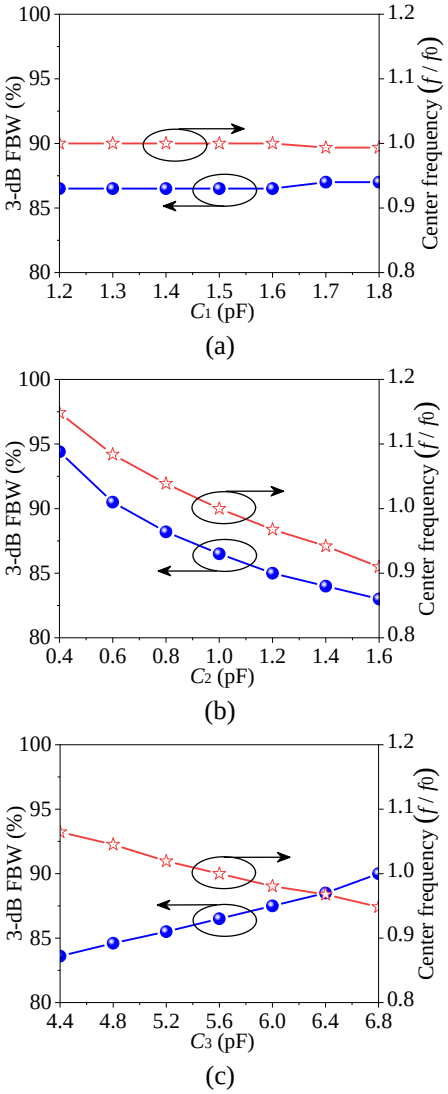

Fig. 4. Effect of capacitance values on theoretical variations of bandwidth and center frequency. (a) C_1 changes; (b) C_2 changes; (c) C_3 changes. (C_1 = 1.5 pF, C_2 = 1.0 pF, C_3 = 5.6 pF, θ_1/θ_2 = 1 and Z_e/Z_o =1.6).

It is found that the bandwidth and center frequency are affected by C_2 and C_3, but not by C_1. This is because C_2 and C_3 change the coupling of the coupled line. However, C_1 will affect impedance matching because it will affect the intensity of the electric field at the feed point.

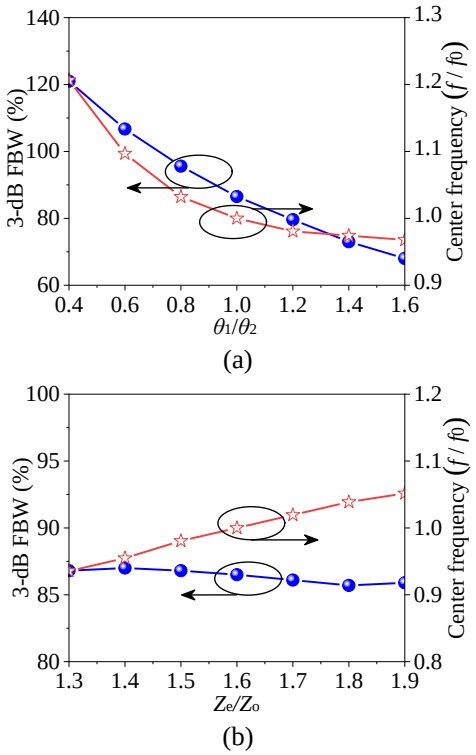

Fig. 5. Effect of the loading position of capacitor and the impedance of coupled line on theoretical variations of bandwidth and center frequency. (a) θ_1/θ_2 changes; (b) Z_e/Z_o changes. (C_1 = 1.5 pF, C_2 = 1.0 pF, C_3 = 5.6 pF, θ_1/θ_2 = 1 and Z_e/Z_o = 1.6).

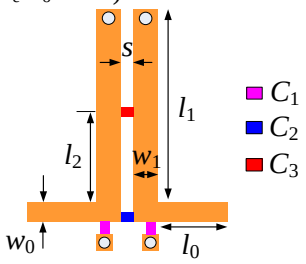

Fig. 6. Layout of the proposed wideband BPF.

C. Parametric study

The layout of the proposed wideband bandpass filter is exhibited in Fig. 6, where the substrate is RO4003C (ε_r = 3.38, h = 0.813 mm, $tan\ \delta$ = 0.0027). In order to further study the performance variation, the parametric study on C_1, C_2, C_3 are displayed in Figs. 7 (a), 7 (b) and 7 (c), respectively. Meanwhile, the parametric study on l_2, w_1, and s_1 are depicted in Figs. 8 (a), 8 (b) and 8 (c), respectively. It can be found from Figs. 7 and 8 that the bandwidth and center frequency are mainly affected by C_2, C_3, l_2, and s, and the out-of-band suppression is mainly changed by C_1, C_2, and s. The bandwidth increases when C_2, l_2, or s is decreased, or C_3 is increased. The center frequency moves upwards with the decrease of C_2, C_3, l_2, or s. The out-of-band suppression becomes better when C_1 is increased, or C_2 or s is decreased.

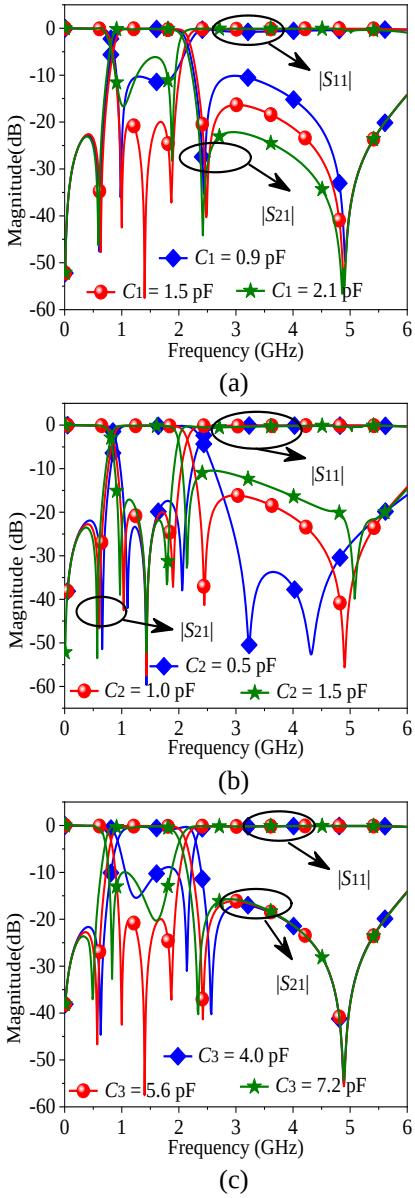

Fig. 7. Simulated responses of the proposed wideband BPF with (a) C_1, (b) C_2, and (c) C_3. (C_1 = 1.5 pF, C_2 = 1.0 pF, C_3 = 5.6 pF, l_2 = 6.7 mm, w_1 = 0.9 mm, and s = 0.58 mm).

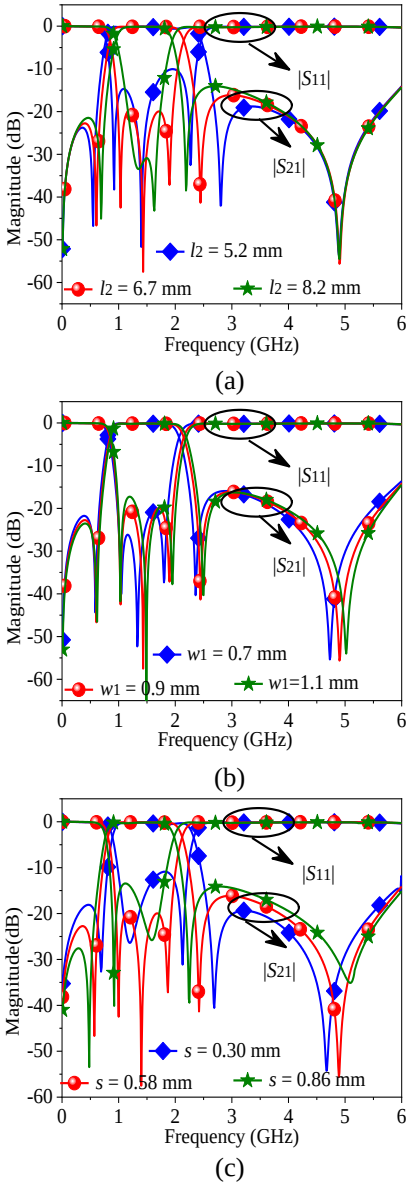

Fig. 8. Simulated responses of the proposed wideband BPF with (a) l_2, (b) w_1, and (c) s. (C_1 = 1.5 pF, C_2 = 1.0 pF, C_3 = 5.6 pF, l_2 = 6.7 mm, w_1 = 0.9 mm, and s = 0.58 mm).

D. Design procedure

According to the above analysis, the design procedure of the proposed wideband BPF is summarized as follows:

Step 1: Get initial C_1, C_2, C_3, θ_1/θ_2, and Z_e/Z_o according to the variation of TPs and TZs in Figs. 2 and 3, and the variation of bandwidth and center frequency in Figs. 4 and 5.

Step 2: Convert the theoretical θ_1/θ_2 and Z_e/Z_o to the dimensions of the coupled line.

Step 3: Obtain final C_1, C_2, C_3, l_2, w_1, and s in Ansoft High Frequency Structure Simulator (HFSS) by slightly tuning them according to their variation in Figs. 7 and 8.

III. PROTOTYPES AND RESULTS

Based on the above analysis, a prototype is implemented with the target of 3-dB FBW of 87% and the center frequency of 1.5 GHz. The final parameters can be obtained from the design procedure and are shown as follows: C_1 = 1.5 pF, C_2 = 1.0 pF, C_3 = 5.6 pF, w_0 = 1.85 mm, w_1 = 0.9 mm, l_0 = 8.0 mm, l_1 = 13.7 mm, l_2 = 4.85 mm, and s = 0.58 mm. The photograph of the proposed wideband BPF is exhibited in Fig. 9 (a).

Figure 9 (b) demonstrates the simulated and measured results of the proposed wideband BPF. The fabricated filter works at the center frequency of 1.47 GHz, which exhibits the 3-dB FBW of 86.5% with a minimum insertion loss of 0.37 dB. Four TZs are loaded at 0 GHz, 0.65 GHz, 2.52 GHz, and 5.09 GHz, while three TPs are loaded at 0.98 GHz, 1.37 GHz, and 1.89 GHz. The overall size of the proposed design is 15.3 mm × 2.38 mm ($0.139\lambda_g \times 0.022\lambda_g = 0.003\lambda_g^2$).

Table 1 lists the performance of this work and the state-of-the-art designs. Compared with the reported microstrip wideband BPF, the proposed design has the advantages of compact size and simple structure.

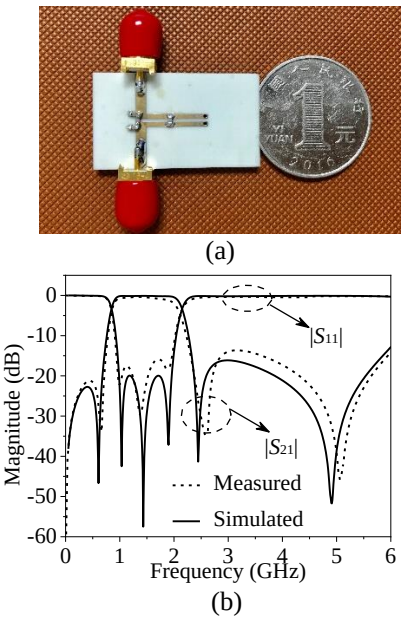

Fig. 9. Photograph and simulation and measured results of the proposed wideband BPF. (a) Photograph and (b) simulation and measured results.

Table 1: Performance comparison between previous state-of-the-art wideband bandpass filters and the proposed design

Ref.	f_0 (GHz)	3-dB FBW (%)	Number of TPs/TZs	Insertion Loss (dB)	Size (λ_g^2)
[1]	2.88	79.33	5/5	0.94	0.271
[7]	3.0	70	5/6	0.49	0.217
[9]	6.0	67.8	5/6	1.3	0.084
[10]	6.85	79.1	6/7	0.81	0.238
[12]	1.91	52.4	2/3	0.3	0.021
[13]	6.9	115.9	7/6	N.A.	0.256
[16]	3.0	80	2/3	0.5	0.013
[17]	0.885	87	3/8	0.66	0.009
[18]	1.0	59.19	4/2	0.64	0.006
This work	1.47	86.5	3/4	0.37	0.003

V. CONCLUSION

A wideband BPF based on capacitor-loaded one-eighth wavelength coupled line is proposed. A compact size of only $0.003\lambda_g^2$ and simple structure can be achieved. Theoretic analysis and parametric study are introduced to guide the practical design. It is believed that the proposed wideband BPF is able to promote the development of the miniaturized wideband wireless communication systems.

ACKNOWLEDGMENT

This work was partially supported by the Nantong Science and Technology Plan Project under Grant JC2018130, Natural Science Foundation of Jiangsu Province, China, under Grant BK20200962, and Natural Science Research Project of Jiangsu Higher Education Institutions under Grant 20KJB510004.

REFERENCES

[1] Y. Wu, L. Cui, W. Zhang, L. Jiao, Z. Zhuang, and Y. Liu, "High performance single-ended wideband and balanced bandpass filters loaded with stepped-impedance stubs," *IEEE Access*, vol. 5, pp. 5972-5981, May 2017.

[2] F. Wei, Z. D. Wang, F. Yang, and X. W. Shi, "Compact UWB BPF with triple-notched bands based on stub loaded resonator," *Electronics Letters*, vol. 49, no. 2, pp. 124-126, Jan. 2013.

[3] R. Li and L. Zhu, "Compact UWB bandpass filter using stub-loaded multiple-mode resonator," *IEEE Microwave and Wireless Components Letters*, vol. 17, no. 1, pp. 40-42, Jan. 2007.

[4] Q. X. Chu, X. H. Wu, and X. K. Tian, "Novel UWB bandpass filters using stub-loaded multiple-mode resonator," *IEEE Microwave and Wireless Components Letters*, vol. 21, no. 8, pp. 403-405, Aug. 2011.

[5] X. Y. Zhang, Y.-W. Zhang, and Q. Xue, "Compact band-notched UWB filter using parallel resonators with a dielectric overlay," *IEEE Microwave and Wireless Components Letters*, vol. 23, no. 5, pp. 252-254, May 2013.

[6] L. Gao, X. Y. Zhang, and Q. Xue, "Compact tri-band bandpass filter using novel eight-mode resonator for 5G WiFi application," *IEEE Microwave and Wireless Components Letters*, vol. 25, no. 10, pp. 660-662, Oct. 2015.

[7] B. Zhang, Y. Wu, and Y. Liu, "Wideband single-ended and differential bandpass filters based on terminated coupled line structures," *IEEE Transactions on Microwave Theory and Techniques*, vol. 65, no. 3, pp. 761-774, Mar. 2017.

[8] X. Xia, X. Cheng, F. Chen, and X. Deng, "Compact UWB bandpass filter with sharp roll-off using APCL structure," *Electronics Letters*, vol. 54, no. 4, pp. 223-225, May 2018.

[9] X. Y. Zhang, X. Dai, H.-L. Kao, B.-H. Wei, Z. Y. Cai, and Q. Xue, "Compact LTCC bandpass filter with wide stopband using discriminating coupling," *IEEE Transactions on Components Packaging and Manufacturing Technology*, vol. 4, no. 4, pp. 656-663, Apr. 2014.

[10] S. W. Ren, H. L. Peng, J. F. Mao, and A. M. Gao, "Compact quasi-elliptic wideband bandpass filter using cross-coupled multiple-mode resonator," *IEEE Microwave and Wireless Components Letters*, vol. 22, no. 8, pp. 397-399, Aug. 2012.

[11] J. Zhou, Y. Chiang, and W. Che, "Wideband bandpass filter based on ring resonator with high selectivity and multiple transmission zeros," *Electronics Letters*, vol. 50, no, 5, pp. 384-386, Feb. 2014.

[12] W. Feng, X. Gao, W. Che, and Q. Xue, "Bandpass filter loaded with open stubs using dual-mode ring resonator," *IEEE Microwave and Wireless Components Letters*, vol. 25, no. 5, pp. 295-297, May 2015.

[13] J. Xu, Y.X. Ji, C. Miao, and W. Wu, "Compact single-/dual-wideband BPF using stubs loaded SIR (SsLSIR)," *IEEE Microwave and Wireless Components Letters*, vol. 23, pp. 338-340, July 2013.

[14] Q. X. Chu and X. K. Tian, "Design of UWB bandpass filter using stepped-impedance stub-loaded resonator," *IEEE Microwave and Wireless Components Letters*, vol. 20, no. 9, pp. 501-503, Sep. 2010.

[15] F. Li, W. Che, L. Gu, and Q. Xue, "Broadband bandpass filter with wide upper stopband using stub-loaded multiple-mode resonators," *Electronics Letters*, vol. 49, no. 13, pp. 818-820, June 2013.

[16] F. Wei, W. T. Li, X. W. Shi, and Q. L. Huang, "Compact UWB bandpass filter with triple-notched bands using triple-mode stepped impedance

resonator," *IEEE Microwave and Wireless Components Letters*, vol. 22, no. 10, pp. 512-514, Oct. 2012.

[17] L. Li and Z. Li, "Side-coupled shorted microstrip line for compact quasi-elliptic wideband bandpass filter design," *IEEE Microwave and Wireless Components Letters*, vol. 20, no. 6, pp. 322-324, June 2010.

[18] J. Xu, Y.-X. Ji, W. Wu, and C. Miao, "Design of miniaturized microstrip LPF and wideband BPF with ultra-wide stopband," *IEEE Microwave and Wireless Components Letters*, vol. 23, no. 8, pp. 397-399, Aug. 2013.

[19] C.-H. Liang and C.-Y. Chang, "Compact wideband bandpass filters using stepped-impedance resonators and interdigital coupling structures," *IEEE Microwave and Wireless Components Letters*, vol. 19, no. 9, pp. 551-553, Sep. 2009.

[20] J. Dong, J. Shi, and K. Xu, "Compact wideband differential bandpass filter using coupled microstrip lines and capacitors," *IEEE Microwave and Wireless Components Letters*, vol. 29, no. 7, pp. 444-446, June 2019.

Jin Shi (M'14) received the B.S. degree from HuaiYin Teachers College, Huai'an City, Jiangsu Province, China, in 2001, the M.S. degree from the University of Electronic Science and Technology of China (UESTC), Chengdu, China, in 2004, and the Ph.D. degree from City University of Hong Kong, in 2011, respectively.

From 2004 to 2006, he was a Research Engineer in Comba working on RF repeater system. During 2007–2008, he was a Research Assistant of the City University of Hong Kong. He joined the Institute for Infocomm Research, Singapore, as a Research Fellow and later served as a Scientist from 2011 to 2013. In 2013, he joined the School of Electronics and Information, Nantong University, China, as a Professor. His current research interests are RF/microwave components and subsystems, differential circuit and antennas, LTCC circuits and antennas.

Shi is the recipient of the IES Prestigious Engineering Achievement Award 2013. He has served as the TPC member and session chair for a number of conferences and a regular reviewer for the IEEE Transactions on Microwave Theory and Techniques, the MWCL, the AWPL, and Electronics Letters, and other publications.

Jiancheng Dong was born in Lianyungang, Jiangsu Province, China, in 1994. He received the B.Sc. degree from Nantong University, Nantong, Jiangsu Province, China, in 2018, where he is currently pursuing the M.S. degree in Electromagnetic Field and Microwave Technology.

His current research interests include RF/microwave components, differential microwave circuits, and tunable circuits.

Kai Xu (M'19) was born in Haian, Jiangsu Province, China, in 1991. He received the B.Sc. degree from Taizhou Institute of Sci. and Tech., Jiangsu Province, China, in 2013, the M.S. degree from the Nantong University, Nantong, Jiangsu Province, China, in 2016, and the Ph.D. degree from the Nantong University, Nantong, Jiangsu Province, China, in 2019, respectively.

From 2015 to 2016, he was a Research Assistant of the Institute for Infocomm Research, Singapore. His current research interests include microwave components, balanced microwave circuits, antennas, and integrated designs.

He has served as a Reviewer for the IEEE access, IEEE MWCL, and IET Electronic Letters, and other publications.

Lingyan Zhang was born in Jiangsu, China in 1991. She received her B.Sc. degree in Applied Physics from Jiangsu University in 2014 and Ph.D. degree in Materials Science and Engineering from Nanjing University of Science and Technology in 2019.

Her research focuses on the microwave transmission system, interaction of ultrafast intense laser with semiconductors and the surface modification of materials.